What do variable magnetic fabrics in gabbros of the Oman ophiolite reveal about lower oceanic crustal magmatism at fast spreading ridges?

Antony Morris[1], Matthew Meyer[1,†], Mark W. Anderson[1] and Christopher J. MacLeod[2]

[1]School of Geography, Earth and Environmental Sciences, Plymouth University, Plymouth PL4 8AA, UK
[2]School of Earth & Ocean Sciences, Cardiff University, Cardiff CF10 3AT, UK
[†]Current address: Petrotechnical Data Systems (PDS Group), Lange Kleiweg 10, 2288 GK Rijswijk, The Netherlands

CITATION: ***Morris, A., Meyer, M., Anderson, M.W. and MacLeod, C.J., 2019. What do variable magnetic fabrics in gabbros of the Oman ophiolite reveal about lower oceanic crustal magmatism at fast spreading ridges? Geology, v. 47, p. 275–278, https:// doi .org /10 .1130 /G45442.1***

ABSTRACT

The magmatic processes responsible for accretion of the lower oceanic crust remain one of the least constrained components of the global seafloor spreading system. Samples of gabbroic rocks recovered by scientific ocean drilling are too limited to allow effective assessment of spatial variations in magmatic flow within in situ lower crust. Extensive exposures of gabbros in ophiolites, on the other hand, provide opportunities to study accretion processes in three-dimensions across wide areas and at a resolution that allows variations in magmatic fabrics through the crust to be quantified. Here we show that magnetic anisotropy provides a reliable proxy for lower crustal magmatic fabrics in the world's largest ophiolite in Oman. Important differences in magnetic fabrics are detected that reflect variations in magmatic processes on a range of scales. Fabrics in layered gabbros are aligned with modal layering and display a consistency in the orientation of maximum principal axes of anisotropy between localities at a regional scale. These fabrics are compatible with subhorizontal preferred alignment of crystals, orthogonal to the inferred orientation of the Oman spreading axis, resulting from magmatic flow or deformation of melt-rich crystal mushes during spreading. In contrast, magnetic anisotropy in foliated gabbros at the top of the lower crust reveals for the first time distinctly different linear and anastomosing fabric styles between localities sampled

at the same pseudostratigraphic level. These differences reflect spatial variations in the style and trajectory of flow in the crystal mush beneath the axial melt lens during upwards melt migration at the spreading axis.

INTRODUCTION

Magmatic accretion of the oceanic crust during seafloor spreading is the foundation of the plate tectonic cycle, forming >60% of the Earth's surface. Seismic imaging at fast spreading rate axes indicates the presence of a thin melt lens at the top of the lower crust (e.g. Detrick et al., 1987; Singh et al., 1998) overlying a broader region inferred to consist of hot crystal mush (Sinton and Detrick, 1992). However, the processes that generate the gabbroic lower crust and the melt transportation system that feeds the axial melt lens remain poorly understood. Conceptual models for lower crustal accretion include: (i) the "gabbro glacier" model, involving downwards ductile flow of the products of crystallization of the melt lens (e.g. Quick and Denlinger, 1993); (ii) the "sheeted sill" model, involving accretion by multiple intrusive events beneath the melt lens without significant vertical transport of the products of crystallization (e.g. Kelemen et al., 1997); (iii) models involving a combination of downward ductile flow and sill intrusion (e.g. Boudier et al., 1996); and (iv) models involving a combination of accretion by multiple intrusions and upwards transportation of melt through the crystal mush to feed the highest level melt body (MacLeod and Yaouancq, 2000; Sun and Lissenberg, 2018). These have fundamentally different implications for the nature of heat and mass transfer at constructive plate margins, e.g. by requiring different depths of hydrothermal circulation to remove magmatic heat and allow crystallization (Maclennan et al., 2005).

Testing these models using lower crustal rocks obtained by scientific ocean drilling has so far proved difficult since significant penetration (> 100 m) has been achieved at only four locations distributed across three oceans (Ildefonse et al., 2014) and drill core samples lack three-dimensional context. In contrast, ophiolites provide extensive, accessible exposures of oceanic lithosphere where spatial variations of fabrics within magmatic products may be analyzed in three-dimensions. In this context, the ~500 km long Oman ophiolite provides an ideal natural laboratory to study lower crustal processes. This Late Cretaceous Neotethyan suprasubduction ophiolite (MacLeod et al., 2013) formed at a fast spreading rate (c. 5-10 cm/a half rate; Rioux et al., 2012) and can therefore provide insights into the style of spreading that produced nearly 50% of the present-day oceanic crust.

Here we use anisotropy of magnetic susceptibility (AMS) as a petrofabric tool to quantify fabrics within lower crustal gabbros of the Oman ophiolite. Previous studies in the Oman and Troodos ophiolites (Yaouancq and MacLeod, 2000; Abelson et al., 2001) and in layered igneous complexes (Ferré et al., 2002) have shown that AMS provides a reliable proxy for the orientation of magmatic fabrics in gabbroic rocks. By comparing fabrics between different sections and pseudostratigraphic levels in the ophiolite, we document variations in fabric style that reflect contrasting magmatic processes between layered gabbros near the base of the crust and foliated gabbros located just below the inferred fossil melt lens, and discuss their implications for models of crustal accretion.

LOWER CRUSTAL GEOLOGY, SAMPLING AND METHODS

Lower oceanic crustal gabbros and underlying mantle peridotites dominate the southern massifs of the Oman ophiolite. We focus on sections in Wadi Abyad (Rustaq massif), at Somrah (Samail massif) and in Wadis Khafifah and Nassif (Ibra massif), where extensive lower crustal exposures occur (Fig. 1). These consist of: (i) layered gabbros, with modal variations in olivine, clinopyroxene and plagioclase on a cm to m scale defining layering that is consistently sub-parallel to the orientation of the Moho; (ii) overlying foliated gabbros in Wadis Abyad and Khafifah, with preferred mineral orientations defining foliations at a high angle to the Moho and steeply plunging lineations; and (iii) varitextured gabbros at the top of the lower crust representing the frozen axial melt lens of the Oman spreading axis (MacLeod and Yaouancq, 2000).

Interpretation of the foliated gabbros has been contentious, with alternative models suggesting that their fabric results from either upwards melt percolation into the overlying axial melt lens (MacLeod and Yaouancq, 2000) or downwards subsidence of crystal mush through the floor of the melt lens in the “gabbro glacier” and related models of lower crustal accretion (Quick and Denlinger, 1993; Boudier et al., 1996; Nicolas et al., 2009).

We report here AMS data from: (i) 20 sites in an across-strike transect within foliated gabbros located immediately beneath the varitextured gabbros in Wadi Abyad; (ii) 19 sites within foliated gabbros in a similar transect located at this same structural level in Wadi Khafifah; and (iii) 18 sites in layered gabbros within Wadis Abyad, Nassif and Khafifah and at Somrah (Fig. 1; see also Fig. DR1 in the GSA Data Repository for geological maps of the sampling localities). Oriented specimens were collected using standard techniques and AMS tensors measured with an AGICO KLY-3S Kappabridge, yielding the magnitude and orientation of the principal axes of low field magnetic susceptibility, $K_{max} \geq K_{int} \geq K_{min}$. Supporting anisotropy of remanence and rock magnetic experiments were also conducted and combined with thin section observations to characterise the source of the AMS signal (see Data Repository for a full description of methods).

RESULTS AND SOURCE OF THE AMS SIGNAL

Details of the anisotropy characteristics of both gabbro types are discussed in the Data Repository and presented in Figs. DR2 – DR5, with specimen-level AMS parameters and principal axes listed in Tables DR1 – DR2 and site-level data in Tables DR3 – DR4. The majority of sites exhibit oblate or triaxial fabrics that correspond closely to the orientation of macroscopic magmatic fabrics observed in the field. K_{max} axes at all sites in the layered gabbros lie in or close to planes of modal layering and also close to magmatic lineations (where visible in the field), with the majority of sites having K_{min} axes close to the pole to layering (Fig. DR3). Within the foliated gabbros (Figs. DR4 and DR5), K_{max} axes at all sites lie in or close to the plane of magmatic foliation, and close to magmatic lineations (observable in the field at only two sites; KF10, KF11).

Bulk susceptibilities in the layered and foliated gabbros (mean values of 2.5×10^{-3} SI and 5.9×10^{-3} SI, respectively) exceed those of the main paramagnetic minerals in these rocks (i.e. clinopyroxene and olivine), requiring a significant but variable ferromagnetic contribution to the AMS signal (Fig. DR2b and c). Corrected anisotropy degrees in the layered gabbros show a broad increase with bulk susceptibility (Fig. DR2c) that results from variations in the ratio of paramagnetic and ferromagnetic contributions to AMS due to changes in modal mineralogy between specimens. This effect is less pronounced in the foliated gabbros that have a more consistent modal composition. Isothermal remanence acquisition experiments show a dominance of low coercivity ferromagnetic grains in both rock types (Fig. DR6), and Curie temperatures determined from thermomagnetic experiments (Fig. DR6), combined with coercivities of remanence of ~25 mT (Meyer, 2015; Morris et al., 2016), indicate that the main ferromagnetic phase is pseudo-single domain, near-stoichiometric magnetite. Distributions of AMS principal axes are mirrored in all cases by those of the anisotropy of partial anhysteretic remanence, that reflects only the fabric component due to magnetite (Fig. DR7). This indicates an absence of inverse fabrics due to single domain magnetite effects (Potter and Stephenson, 1988). Hence AMS K_{max} and K_{min} axes may be interpreted as magnetic lineations and poles to magnetic foliations, respectively. Coaxiality of fabrics across specimens with varying susceptibilities indicates no significant difference in the orientation of the paramagnetic silicate and ferromagnetic magnetite contributions to the AMS signal.

Photomicrographs of oriented thin sections cut in the K_{max}/K_{min} plane are shown in Fig. 2 (with the orientation of K_{max} axes indicated by red arrows). Both layered and foliated gabbros show a lack of crystal plastic or brittle fabrics. Instead, clear magmatic fabrics defined by pronounced shape preferred orientations of plagioclase, clinopyroxene and olivine are present that are consistently oriented parallel to K_{max} axes (Fig. 2), with the majority of crystal long-axes aligned with K_{max} to within 20° (Meyer, 2015). Interstitial magnetite of primary magmatic origin is usually rare in both units. Instead, magnetite inclusions are present along clinopyroxene cleavage planes as an exsolution product formed during cooling. Fine-grained secondary magnetite is also distributed along fractures that are aligned with the long axes of olivine crystals that have undergone variable degrees of serpentinization (Fig. 2). Olivine crystals are also surrounded by alteration rims of very fine-grained acicular tremolite, chlorite and minor opaques.

These observations, together with the close alignment of principal axes of anisotropy with magmatic layering, foliations and lineations measured in the field, demonstrate that AMS in these rocks provides a reliable proxy for the orientation of primary magmatic silicate fabrics formed during crustal accretion, even in specimens containing secondary magnetite (as reported previously by Yaouancq and MacLeod, 2000).

DISCUSSION

Regional Scale Consistency In Layered Gabbro Fabrics

Layered gabbros from all four localities share a common ENE-WSW-trending, subhorizontal orientation of K_{max} axes and sub-vertical orientation of K_{min} axes (Fig. 3A), demonstrating a consistency of magmatic fabrics at a regional scale. The magnetic lineation results from a subhorizontal preferred alignment of crystals, orthogonal to the inferred NNW present day orientation of the Oman axis (Fig. 1) and in close agreement with the trajectories of mineral lineations in gabbros and peridotites mapped across the ophiolite (Nicolas et al., 2000) (Fig. 1). Since significant crystal plastic deformation is absent in the layered gabbros, this preferred alignment must reflect magmatic flow during accretion or, more likely, post-intrusive deformation of a melt-rich crystal mush resulting from mechanical coupling with the underlying mantle during spreading (Nicolas et al., 1994). A dominance of oblate and triaxial AMS fabrics at this level is also consistent with a significant pure shear, compaction-related component to the fabric in these rocks. Our AMS evidence for axis-normal magmatic flow/deformation in the fast spreading Oman ophiolite contrasts with along-axis flow revealed using AMS in the lower crust and sheeted dyke complex of the slow spreading rate Troodos ophiolite (Staudigel et al., 1992; Abelson et al., 2001). This difference reflects a fundamental dependence of magmatic supply at ridge axes on spreading rate (Lin and Morgan, 1992), whereby fast/slow spreading axes are characterised by continuous/discontinuous supply of melt from the mantle along their length, respectively.

Foliated Gabbro Fabrics And Their Implications For Magmatic Accretion Processes

In contrast to the layered gabbros, AMS fabrics in the foliated gabbros just below the fossil axial melt lens vary in character between localities (Fig. 3). In the Wadi Abyad transect, K_{max} axes are highly clustered and plunge steeply within the macroscopic magmatic foliation observed in the field at all sampling sites, with K_{min} axes clustered near the pole to the foliation (Fig. 3B). Fabrics are distinctly different in Wadi Khafifah, however, where K_{max} axes define a girdle distribution within the foliation plane (with K_{min} axes again clustering around the foliation pole; Fig. 3C). This distribution reflects variability across a range of scales. Magmatic alignment of crystals at the specimen scale defines a texture with plagioclase crystals anastomosing between clinopyroxene and olivine phenocrysts (Fig. 2), with AMS at this scale representing the average orientation of this magmatic fabric. At the site scale, AMS fabrics display clustering of K_{max} axes within the macroscopic foliation (Fig. DR5), indicating consistency of the average orientation of this anastomosing fabric style across areas of ~2.0 m^2. At the largest, transect scale (c. 500-700 m^2), fabrics vary in average orientation between sites (Fig. 3; Fig. DR5), with K_{max} axes representing preferred crystal alignments that range from subhorizontal to steeply plunging within the plane of the foliation.

In gabbro glacier and hybrid models of lower crustal accretion (Quick and Denlinger, 1993; Boudier et al., 1996; Nicolas et al., 2009), steep fabrics in the foliated gabbros form via downwards subsidence and steepening of initially horizontal cumulate layers at the base of the axial melt lens. However, presence of a steep fabric of magmatic origin to within a few meters of the inferred melt lens (MacLeod and Yaouancq, 2000) and a lack of systematic changes with depth in the strength of plagioclase lattice preferred orientations (Van Tongeren et al., 2015) are not consistent with the progressive steepening of fabrics predicted by gabbro glacier models. Our analysis for the first time demonstrates significant spatial variations in fabrics in the foliated gabbros at this level (Fig. 3), that are also incompatible with subsidence through the floor of the melt lens. Instead, our observations are more consistent with variations in the trajectory of flow in the crystal mush beneath the melt lens during upwards migration of magma via porous flow, with focused channelized flow at Wadi Abyad and more distributed melt percolation (including components of upwards and lateral flow) at Wadi Khafifah. The style of fabric frozen into the gabbros below the axial melt lens may be expected to vary as a function of proximity to the focus of melt supply across the ridge (Fig. 3) or in response to differences in melt supply along the axis. Such along-axis differences have been mapped by seismic reflection experiments along the East Pacific Rise (Singh et al., 1998), with pure melt zones inferred to correspond to regions of fresh supply of magma from the mantle and mush zones inferred to have undergone cooling and crystallization and to be more evolved (Singh et al., 1998). In this context, we note that foliated gabbros in Wadi Khafifah are more evolved than those in Wadi Abyad (MacLeod and Yaouancq, 2000; Garrido et al., 2001; MacLeod, unpublished data) supporting a connection between melt supply and fabric development in fast spreading rate magmatic systems.

ACKNOWLEDGEMENTS

We thank Mohamed Alaraimi (Sultanate of Oman Ministry of Commerce and Industry, Directorate General of Minerals) for permission to undertake field sampling in Oman, and Stuart Gilder for allowing us to use the University of Munich “Sushi-Bar” system for remanence anisotropy analyses. Stereonets were produced using OSXStereonet (Cardozo and Allmendinger, 2013). We thank C. Mac Niocaill, G. Ceuleneer and an anonymous reviewer for constructive reviews.

REFERENCES CITED

Abelson, M., Baer, G., and Agnon, A., 2001, Evidence from gabbro of the Troodos ophiolite for lateral magma transport along a slow-spreading mid-ocean ridge.: Nature, v. 409, p. 72–5, doi: 10.1038/35051058.

Boudier, F., Nicolas, A., and Ildefonse, B., 1996, Magma chambers in the Oman ophiolite: fed from the top and the bottom: Earth and Planetary Science Letters, v. 144, p. 239–250, doi: 10.1016/0012-821X(96)00167-7.

Cardozo, N., and Allmendinger, R.W., 2013, Spherical projections with OSXStereonet: Computers and Geosciences, v. 51, p. 193–205, doi: 10.1016/j.cageo.2012.07.021.

Detrick, R.S., Buhl, P., Vera, E., Mutter, J., Orcutt, J., Madsen, J., and Brocher, T., 1987, Multi-channel seismic imaging of a crustal magma chamber along the East Pacific Rise: Nature, v. 326, p. 35–41, doi: 10.1038/326035a0.

Ferré, E.C., Bordarier, C., and Marsh, J.S., 2002, Magma flow inferred from AMS fabrics in a layered mafic sill, Insizwa, South Africa: Tectonophysics, v. 354, p. 1–23, doi:

10.1016/S0040-1951(02)00273-1.

Garrido, C.J., Kelemen, P.B., and Hirth, G., 2001, Variation of cooling rate with depth in lower crust formed at an oceanic spreading ridge: Plagioclase crystal size distributions in gabbros from the Oman ophiolite: Geochemistry, Geophysics, Geosystems, v. 2, doi: 10.1029/2000GC000136.

Ildefonse, B., Abe, N., Godard, M., Morris, A., Teagle, D.A.H., and Umino, S., 2014, Formation and Evolution of Oceanic Lithosphere: New Insights on Crustal Structure and Igneous Geochemistry from ODP/IODP Sites 1256, U1309, and U1415: v. 7, doi: 10.1016/B978-0-444-62617-2.00017-7.

Kelemen, P.B., Koga, K., and Shimizu, N., 1997, Geochemistry of gabbro sills in the crust-mantle transition zone of the Oman ophiolite: implications for the origin of the oceanic lower crust: Earth and Planetary Science Letters, v. 146, p. 475–488, doi: 10.1016/S0012-821X(96)00235-X.

Lin, J., and Morgan, J.P., 1992, The spreading rate dependence of three-dimensional mid-ocean ridge gravity structure: Geophysical Research Letters, v. 19, p. 13–16, doi: 10.1029/91GL03041.

Maclennan, J., Hulme, T., and Singh, S.C., 2005, Cooling of the lower oceanic crust: Geology, v. 33, p. 357–360, doi: 10.1130/G21207.1.

MacLeod, C.J., and Yaouancq, G., 2000, A fossil melt lens in the Oman ophiolite: Implications for magma chamber processes at fast spreading ridges: Earth and Planetary Science Letters, v. 176, p. 357–373, doi: 10.1016/S0012-821X(00)00020-0.

MacLeod, C. J., Lissenberg, C. J. and Bibby, L. E., 2013. “Moist MORB” axial magmatism in the Oman ophiolite: The evidence against a mid-ocean ridge origin, Geology, 41, 459-462

Meyer, M., 2015, Magnetic fabric, palaeomagnetic and structural investigation of the accretion of lower oceanic crust using ophiolitic analogues: PhD Thesis, University of Plymouth, 335 p.

Morris, A., Meyer, M., Anderson, M.W., and MacLeod, C.J., 2016, Clockwise rotation of the entire Oman ophiolite occurred in a suprasubduction zone setting: Geology, v. 44, doi: 10.1130/G38380.1.

Nicolas, A., Boudier, F., and France, L., 2009, Subsidence in magma chamber and the development of magmatic foliation in Oman ophiolite gabbros: Earth and Planetary Science Letters, v. 284, p. 76–87, doi: 10.1016/j.epsl.2009.04.012.

Nicolas, A., Boudier, F., and Ildefonse, B., 1994, Evidence from the Oman ophiolite for active mantle upwelling beneath a fast-spreading ridge: Nature, v. 370, p. 51–53, doi:

10.1038/370051a0.

Nicolas, A., Bouldier, F., Ildefonse, B., and Ball, E., 2000, Accretion of Oman and United Arab Emirates ophiolite - Discussion of a new structural map: Marine Geophysical Researches, v. 21, p. 147–179, doi: 10.1023/A:1026769727917.

Potter, D.K., and Stephenson, A., 1988, Single-domain particles in rocks and magnetic fabric analysis: Geophysical Research Letters, v. 15, p. 1097–1100, doi: 10.1029/GL015i010p01097.

Quick, J.E., and Denlinger, R.P., 1993, Ductile deformation and the origin of layered gabbro in ophiolites: Jour. Geophys. Res., v. 98, p. 14015–14027, doi: 10.1029/93JB00698.

Rioux, M., Bowring, S., Kelemen, P., Gordon, S., Dudás, F., and Miller, R., 2012, Rapid crustal accretion and magma assimilation in the Oman-U . A . E . ophiolite : High precision U-Pb zircon geochronology of the gabbroic crust: v. 117, p. 1–12, doi: 10.1029/2012JB009273.

Singh, S.C., Kent, G.M., Collier, J.S., Harding, A.J., and Orcutt, J.A., 1998, Melt to mush variations in crustal magma properties along the ridge crest at the southern East Pacific Rise: Nature, v. 394, p. 874–878, doi: 10.1038/29740.

Sinton, J.M., and Detrick, R.S., 1992, Midocean ridge magma chambers: Journal of Geophysical Research-Solid Earth, v. 97, p. 197–216, doi: 10.1029/91jb02508.

Staudigel, H., Gee, J., Tauxe, L., and Varga, R.J., 1992, Shallow intrusive directions of intrusive dikes in the Troodos ophiolite: anisotropy of magnetic susceptibility and structural data: Geology, v. 20, p. 841–844, doi: 10.1130/0091-7613(1992)020<0841.

Sun, C., and Lissenberg, C.J., 2018, Formation of fast-spreading lower oceanic crust as revealed by a new Mg–REE coupled geospeedometer: Earth and Planetary Science Letters, v. 487, p. 165–178, doi: 10.1016/j.epsl.2018.01.032.

Van Tongeren, J. A., Hirth, G. and Kelemen, P. B., 2015, Constraints on the accretion of the gabbroic lower oceanic crust from plagioclase lattice preferred orientation in the Samail ophiolite: Earth and Planetary Science Letters, v. 427, p. 249–261, doi: 10.1016/j.epsl.2015.07.001.

Yaouancq, G., and MacLeod, C.J., 2000, Petrofabric Investigation of Gabbros from the Oman Ophiolite: Comparison between AMS and Rock Fabric: Marine Geophysical Researches, v. 21, p. 289–305, doi: 10.1023/A:1026774111021.

FIGURE CAPTIONS:

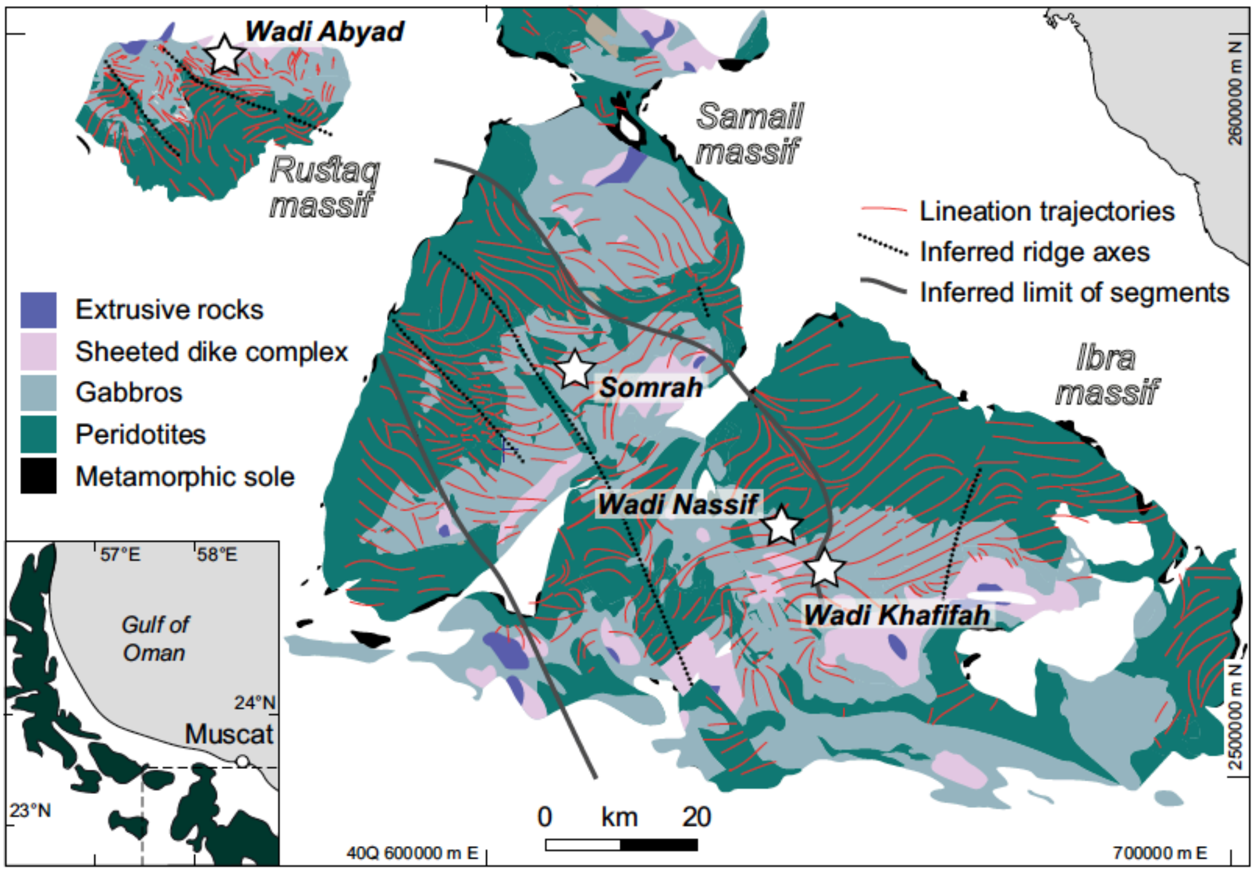

Figure 1. Geological map of the southern massifs of the Oman ophiolite showing the location of sampling localities and trajectories of solid-state flow in mantle peridotites and magmatic flow in lower crustal gabbros (modified from Nicolas et al., 2000)

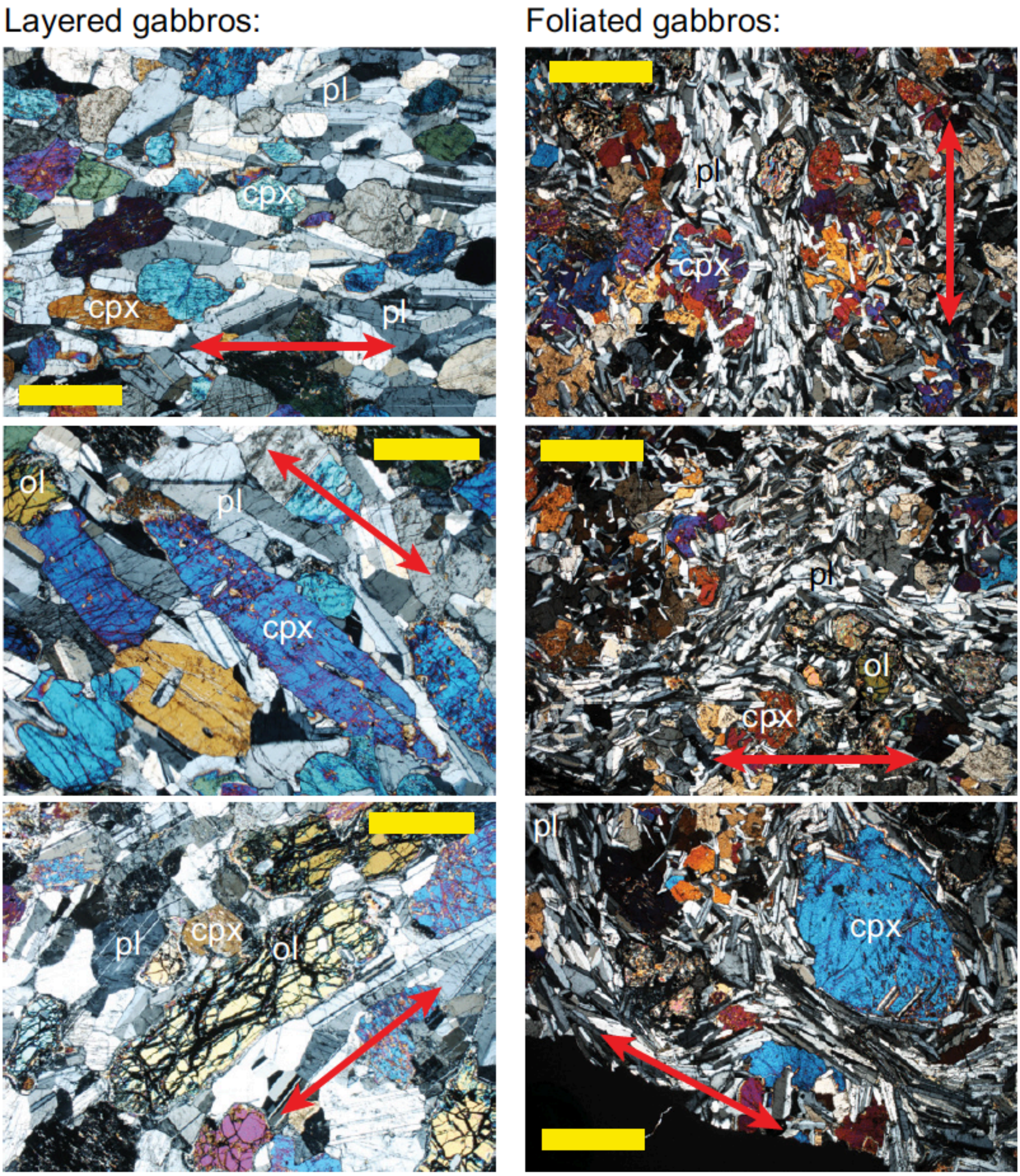

Figure 2. Photomicrographs of thin sections of layered and foliated gabbros from the Oman ophiolite, showing correlation of K_{max} axes (red arrows) with preferred orientations of silicate crystals and of secondary magnetite in olivine crystals (bottom left). Yellow scale bars = 1.0 mm.

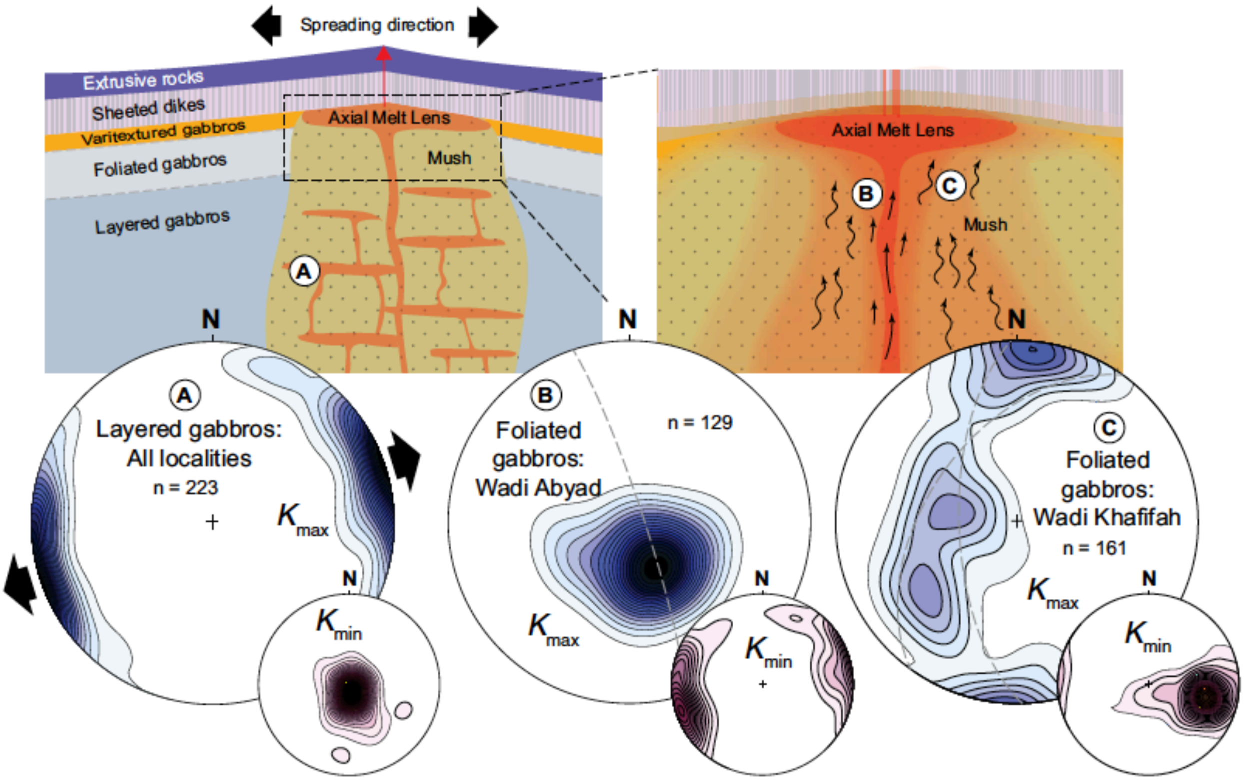

Figure 3. Summary of AMS results from the Oman ophiolite lower crustal sequences. Large/small stereonets show Kamb contoured distributions of K_{max}/K_{min} principal susceptibility axes, respectively, combining specimen level data from all sites. A: Layered gabbros after rotating modal layering at each site to the horizontal. B and C: Foliated gabbros after restoring the Moho at each locality to the horizontal. Schematic diagrams of crustal structure after Sun and Lissenberg (2018) and MacLeod and Yaouancq (2000).

What do variable magnetic fabrics in gabbros of the Oman ophiolite reveal about lower oceanic crustal magmatism at fast spreading ridges?

Antony Morris[1], Matthew Meyer[1,†], Mark W. Anderson[1] and Christopher J. MacLeod[2]

[1]School of Geography, Earth and Environmental Sciences, Plymouth University, Plymouth PL4 8AA, UK
[2]School of Earth & Ocean Sciences, Cardiff University, Cardiff CF10 3AT, UK
[†]Current address: Petrotechnical Data Systems (PDS Group), Lange Kleiweg 10, 2288 GK Rijswijk, The Netherlands

DATA REPOSITORY TEXT

METHODS

Samples were collected using a portable rock drill and the orientation of drill cores measured using both magnetic and sun compasses. Additional oriented hand samples were collected at some sites and drilled back in the laboratory. The orientations of macroscopic magmatic fabrics in the field (modal layering and magmatic foliations/lineations) were determined from multiple measurements at each site. In the laboratory, all core samples were sliced into standard (11 cm^3) cylindrical specimens.

We measured the anisotropy of low-field magnetic susceptibility (AMS) of specimens using an AGICO KLY-3S Kappabridge. AMS is a petrofabric tool that reflects the preferred orientation of grains, grain distributions and/or the crystal lattices of minerals that contribute to the magnetic susceptibility of a rock (e.g. Tarling and Hrouda, 1993; Borradaile and Jackson, 2004). AMS corresponds to a second order tensor that may be represented by an ellipsoid specified by the orientation and magnitude of its principal axes (K_{max}, K_{int} and K_{min}, being the maximum, intermediate, and minimum susceptibility axes respectively) (Tarling and Hrouda, 1993). The AMS of a rock may result from contributions from diamagnetic, paramagnetic and ferromagnetic minerals. Susceptibility tensors and associated eigenvectors and eigenvalues were calculated using AGICO Anisoft 4.2 software. The relative magnitude of the susceptibility axes defines the shape of the AMS ellipsoid, which can be: (1) isotropic ($K_{min} = K_{int} = K_{max}$) when crystals are not aligned preferentially; (2) oblate ($K_{min} << K_{int} \approx K_{max}$) when crystal alignment defines a foliation plane; (3) triaxial ($K_{min} < K_{int} < K_{max}$); or (4) prolate ($K_{min} \approx K_{int} << K_{max}$) when crystal alignment defines a lineation. Here we describe the strength of anisotropy using the corrected anisotropy degree (P_J; Jelínek, 1981), where $P_J = 1.0$ indicates an isotropic fabric and, e.g., $P_J = 1.05$ indicates 5% anisotropy. The shape of the ellipsoid is described by the shape parameter (T), where $-1.0 < T < 1.0$ with positive/negative values of T indicate oblate/prolate fabrics respectively (Jelínek, 1981).

Rock magnetic experiments were performed to investigate the nature of the ferromagnetic minerals contributing to the AMS. Curie temperatures were determined from the high-temperature (20–700°C) variation of magnetic susceptibility of representative samples, measured using an AGICO KLY-3S Kappabridge coupled with an AGICO CS-3 high-temperature furnace apparatus. Curie temperatures were determined from these data using the method of Petrovský and Kapička (2006).

Isothermal remanent magnetization (IRM) acquisition experiments were conducted on representative samples using a Molspin pulse magnetizer to apply peak fields up to 800 mT with resulting IRMs measured using an AGICO JR6A fluxgate spinner magnetometer.

Finally, observations of oriented thin sections were used to further establish the source of the AMS signal. These were prepared by calculating the orientation of the plane containing the K_{max} and K_{min} principal axes relative to the fiducial line for each specimen.

Thin section billets were then cut parallel to these planes, maintaining reference marks for the orientation of K_{max} and K_{min} axes for transfer to the thin section slides.

ANISOTROPY CHARACTERISTICS

The complete dataset of specimen-level AMS parameters and principal axes is provided in Tables DR1 and DR2. The relationship between P_J and T is shown in Fig. DR2a, with 67% of specimens exhibiting oblate fabrics (median value of T = 0.25) and P_J ranging from 1.01 to 1.46 (median value of 1.09).

At a higher (site) level, clustering of specimen K_{max} and K_{min} axes define the magnetic lineation and the pole to the magnetic foliation, respectively. Oblate fabrics are characterized by clustered K_{min} axes orthogonal to girdle distributions of K_{max} and K_{int} axes, whereas prolate fabrics by clustered K_{max} axes orthogonal to girdle distributions of K_{int} and K_{min} axes. In triaxial fabrics, the three principal susceptibility axes form distinct groups. Site-level distributions of principal AMS axes in geographic coordinates are shown in Figs. DR3-5, with site mean anisotropy parameters listed in Tables DR3 and DR4. The majority of sites in the layered gabbros (Fig. DR3) exhibit triaxial or oblate fabrics, with prolate fabrics only present at three sites (WA10, WA11 and SR02). In all cases, K_{max} axes lie in or close to the plane of modal layering measured in the field, with the majority of sites having K_{min} axes close to the pole to layering. Macroscopic magmatic lineations were visible in the field at nine layered gabbro sites and in all cases lie close to the associated K_{max} axes (Fig. DR3). Within the foliated gabbros (Figs. DR4 and DR5), 19 sites in Wadi Abyad and 11 sites in Wadi Khafifah exhibit triaxial fabrics. K_{max} axes at all sites lie in or close to the plane of magmatic foliation, and close to magmatic lineations (observable in the field at only two sites; KF10, KF11).

DATA REPOSITORY – REFERENCES

Borradaile, G.J., and Jackson, M., 2004, Anisotropy of magnetic susceptibility (AMS): magnetic petrofabrics of deformed rocks: Geological Society, London, Special Publications, v. 238, p. 299–360, doi: 10.1144/GSL.SP.2004.238.01.18.

Garrido, C.J., Kelemen, P.B., and Hirth, G., 2001, Variation of cooling rate with depth in lower crust formed at an oceanic spreading ridge: Plagioclase crystal size distributions in gabbros from the Oman ophiolite: Geochemistry, Geophysics, Geosystems, v. 2, doi: 10.1029/2000GC000136.

Jelinek, V., 1981, Characterization of the magnetic fabric of rocks: Tectonophysics, v. 79, p. 63–67, doi: 10.1016/0040-1951(81)90110-4.

MacLeod, C.J., and Yaouancq, G., 2000, A fossil melt lens in the Oman ophiolite: Implications for magma chamber processes at fast spreading ridges: Earth and Planetary Science Letters, v. 176, p. 357–373, doi: 10.1016/S0012-821X(00)00020-0.

Petrovský, E., and Kapička, A., 2006, On determination of the Curie point from thermomagnetic curves: Journal of Geophysical Research: Solid Earth, v. 111, p. n/a-n/a, doi: 10.1029/2006JB004507.

Tarling, D.H. (Donald H., and Hrouda, F. (František), 1993, The magnetic anisotropy of rocks: Chapman & Hall, 217 p.

DATA REPOSITORY FIGURE AND TABLE CAPTIONS:

Figure DR1. Geological maps of sampling localities in the Oman ophiolite. A: Wadi Abyad (modified from MacLeod and Yaouancq, 2000); B: Wadi Khafifah (modified from Garrido et al., 2001); C: Wadi Nassif; and D: Somrah.

Figure DR2. Summary of anisotropy of magnetic susceptibility parameters for gabbros of the Oman ophiolite.

Figure DR3. Site-level distributions of AMS principal axes in layered gabbros of the Oman ophiolite. Gray dashed great circles = the orientation of modal layering; white stars = orientation of macroscopic magmatic lineation (where present).

Figure DR4. Site-level distributions of AMS principal axes in foliated gabbros exposed in Wadi Abyad of the Oman ophiolite. Gray dashed great circles = the orientation of macroscopic magmatic foliation.

Figure DR5. Site-level distributions of AMS principal axes in foliated gabbros exposed in Wadi Khafifah of the Oman ophiolite. Gray dashed great circles = the orientation of macroscopic magmatic foliation; white stars = orientation of macroscopic magmatic lineation (where present).

Figure DR6. Representative examples of isothermal remanent magnetization acquisition curves and of the variation of low field magnetic susceptibility with temperature for lower crustal rocks from the Oman ophiolite, consistent with presence of magnetite as the main ferromagnetic phase present. Tc = Curie temperature, calculated using the inverse susceptibility method (Petrovský and Kapička, 2006).

Figure DR7. Comparison of anisotropies of partial anhysteretic remanence (ApARM) and magnetic susceptibility (AMS) demonstrating presence of normal magnetic fabrics in lower crustal rocks of the Oman ophiolite.

Table DR1. Specimen-level anisotropy of magnetic susceptibility data from layered gabbros of the Oman ophiolite.

Table DR2. Specimen-level anisotropy of magnetic susceptibility data from foliated gabbros of the Oman ophiolite.

Table DR3. In situ site-level anisotropy of magnetic susceptibility results from layered gabbros of the Oman ophiolite.

Table DR4. In situ site-level anisotropy of magnetic susceptibility results from foliated gabbros of the Oman ophiolite.

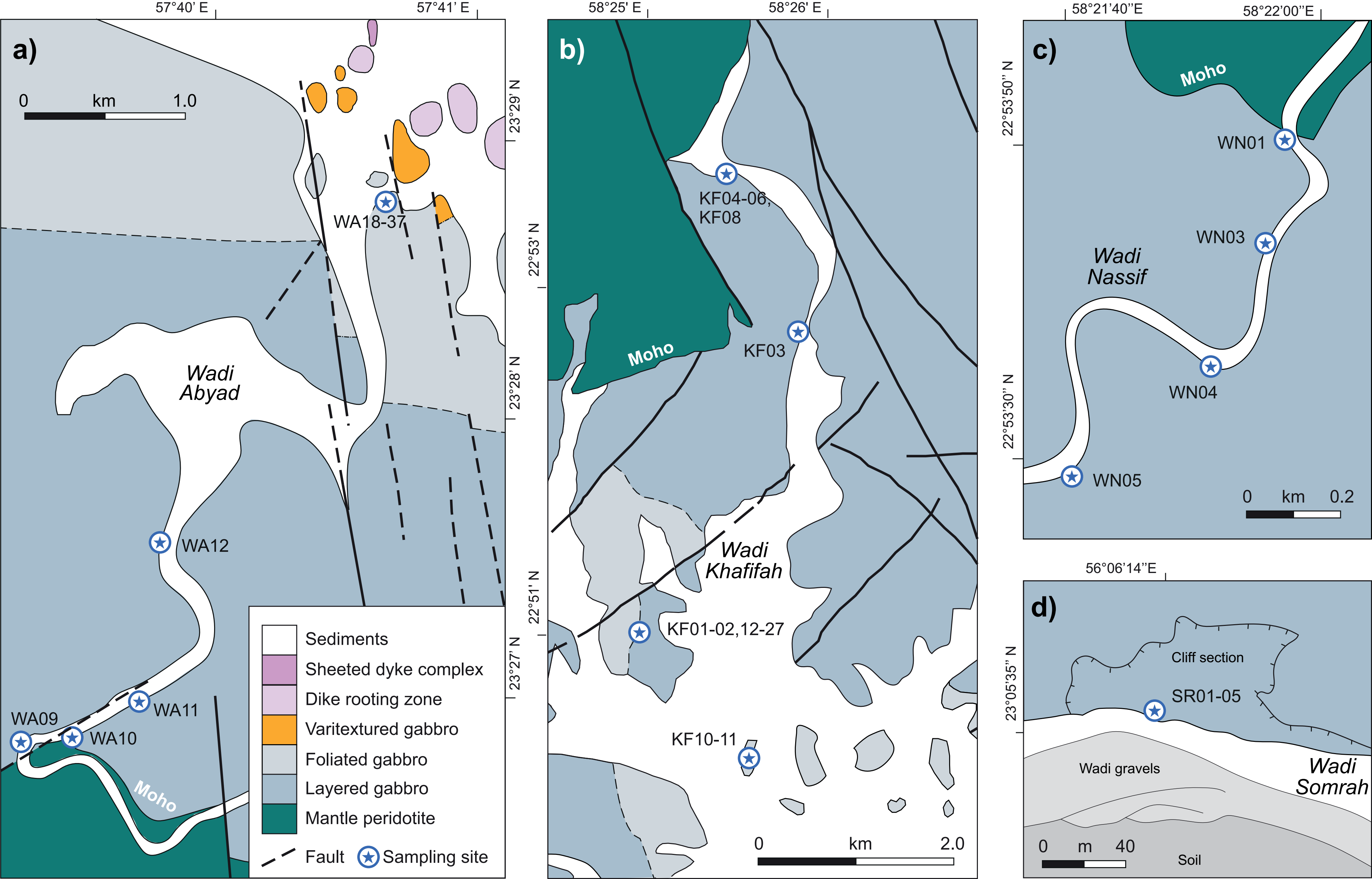
a)
57°40' E
57°41' E
23°29' N
23°28' N
23°27' N
0
km
1.0
WA18-37
Wadi
Abyad
WA12
WA11
WA09
WA10
Moho
Sediments
Sheeted dyke complex
Dike rooting zone
Varitextured gabbro
Foliated gabbro
Layered gabbro
Mantle peridotite
Fault
Sampling site
b)
58°25' E
58°26' E
22°53' N
22°51' N
KF04-06,
KF08
KF03
Moho
Wadi
Khafifah
KF01-02,12-27
KF10-11
0
km
2.0
c)
58°21'40''E
58°22'00''E
22°53'50'' N
22°53'30'' N
Moho
WN01
WN03
Wadi
Nassif
WN04
WN05
0
km
0.2
d)
56°06'14''E
23°05'35'' N
Cliff section
SR01-05
Wadi gravels
Wadi
Somrah
0
m
40
Soil

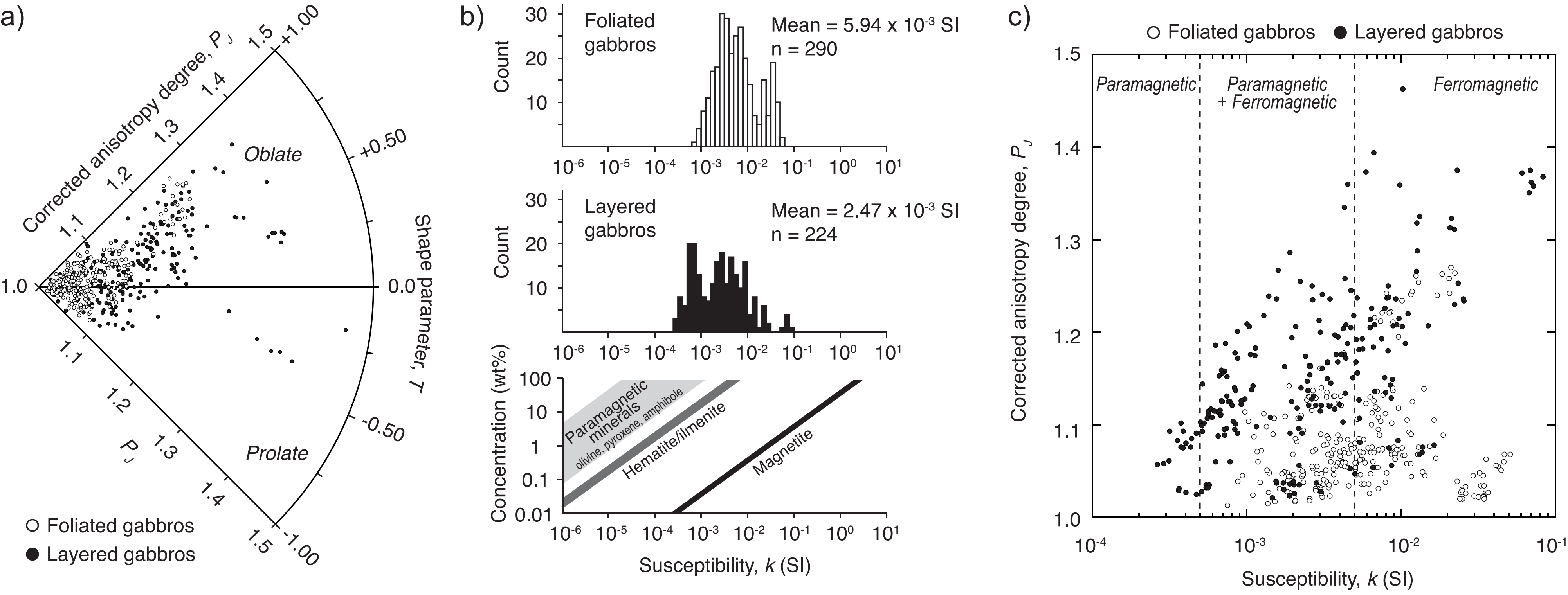
a)
Corrected anisotropy degree, P_J
Shape parameter, T
Oblate
Prolate
P_J
Foliated gabbros
Layered gabbros
b)
Foliated gabbros
Mean = 5.94 x 10^-3 SI
n = 290
Layered gabbros
Mean = 2.47 x 10^-3 SI
n = 224
Count
Concentration (wt%)
Paramagnetic minerals
olivine, pyroxene, amphibole
Hematite/ilmenite
Magnetite
Susceptibility, k (SI)
c)
Foliated gabbros
Layered gabbros
Paramagnetic
Paramagnetic + Ferromagnetic
Ferromagnetic
Corrected anisotropy degree, P_J
Susceptibility, k (SI)

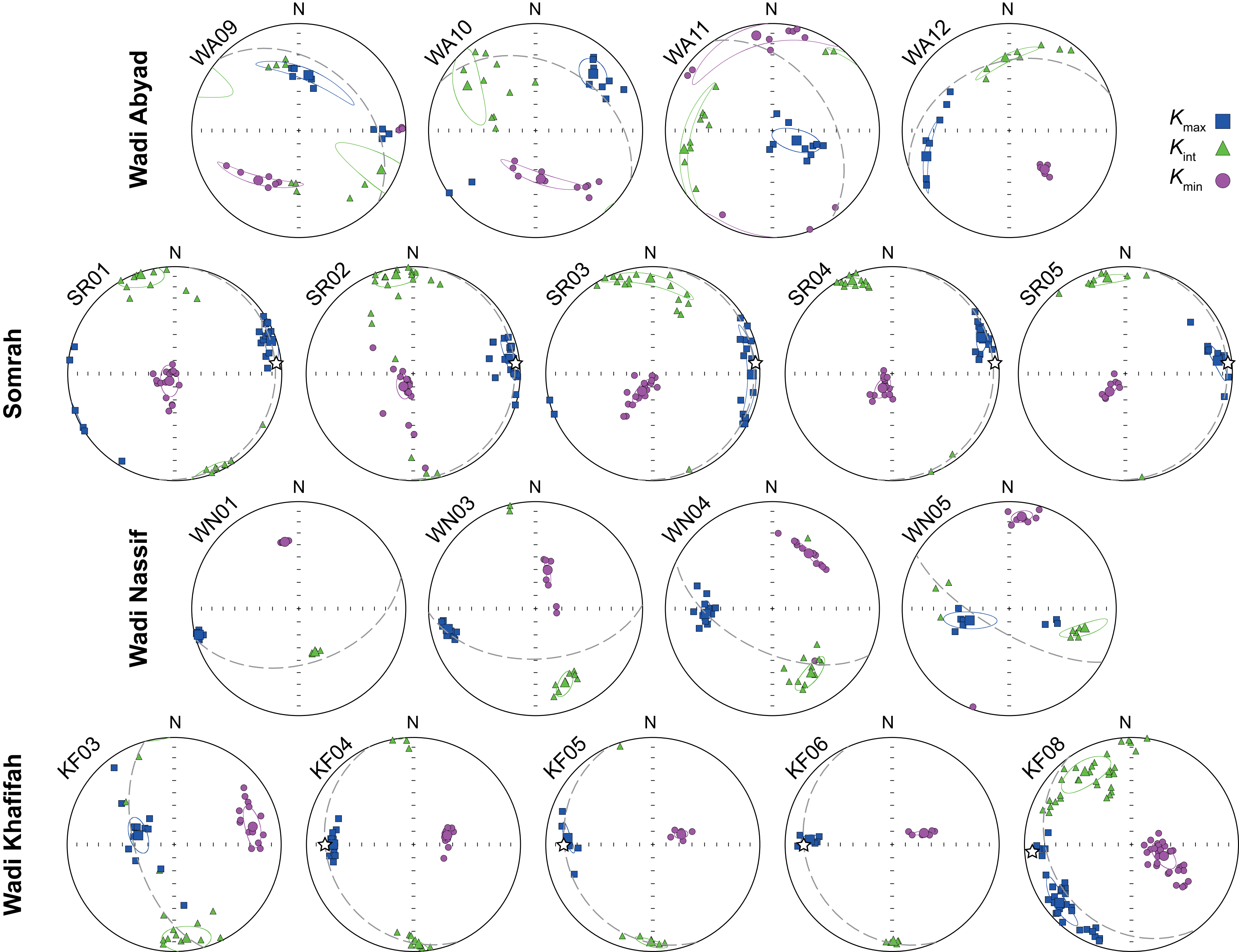

Wadi Abyad
Somrah
Wadi Nassif
Wadi Khafifah
N
WA09
WA10
WA11
WA12
SR01
SR02
SR03
SR04
SR05
WN01
WN03
WN04
WN05
KF03
KF04
KF05
KF06
KF08
K_{max}
K_{int}
K_{min}

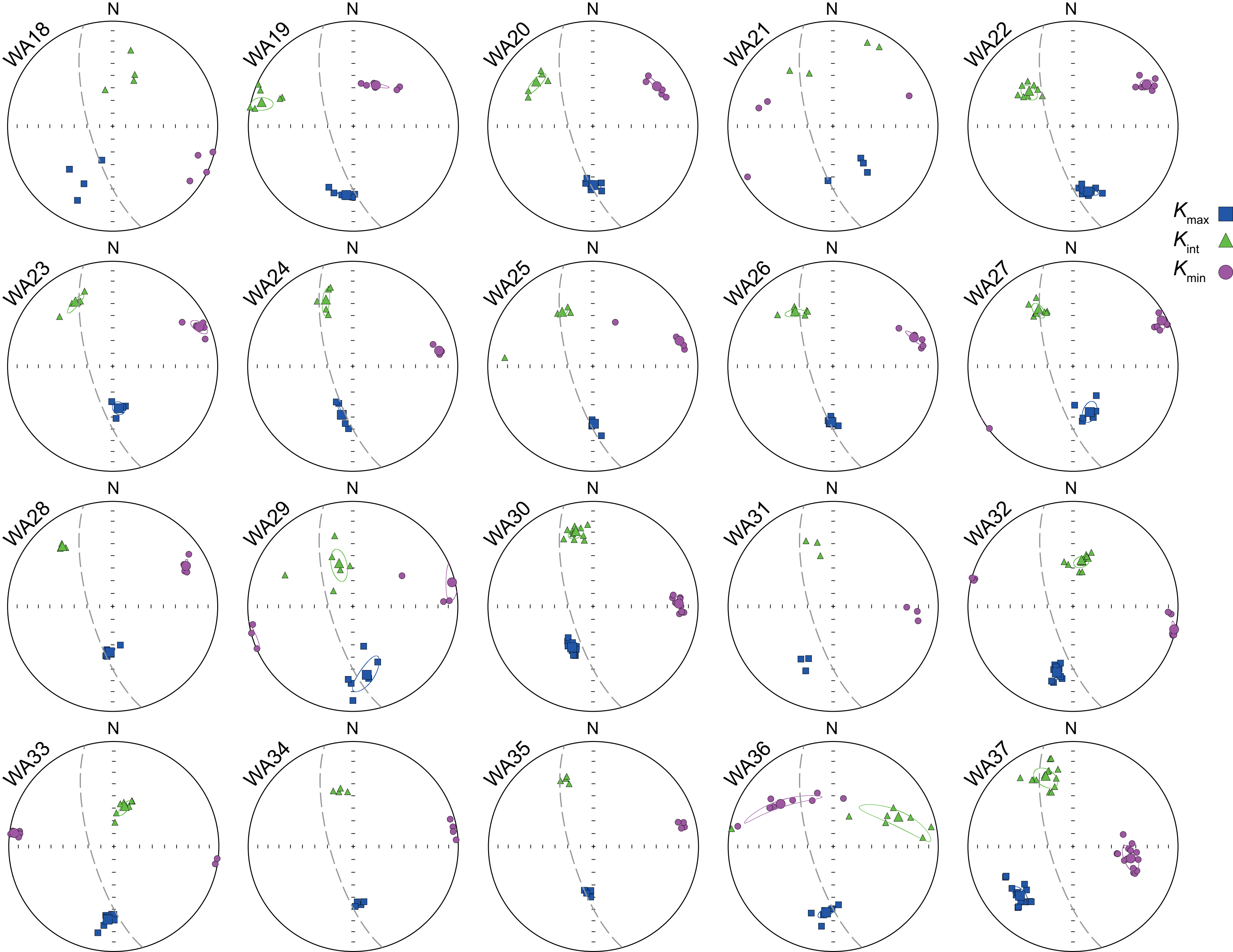

WA18
WA19
WA20
WA21
WA22
WA23
WA24
WA25
WA26
WA27
WA28
WA29
WA30
WA31
WA32
WA33
WA34
WA35
WA36
WA37
N
K_{max}
K_{int}
K_{min}

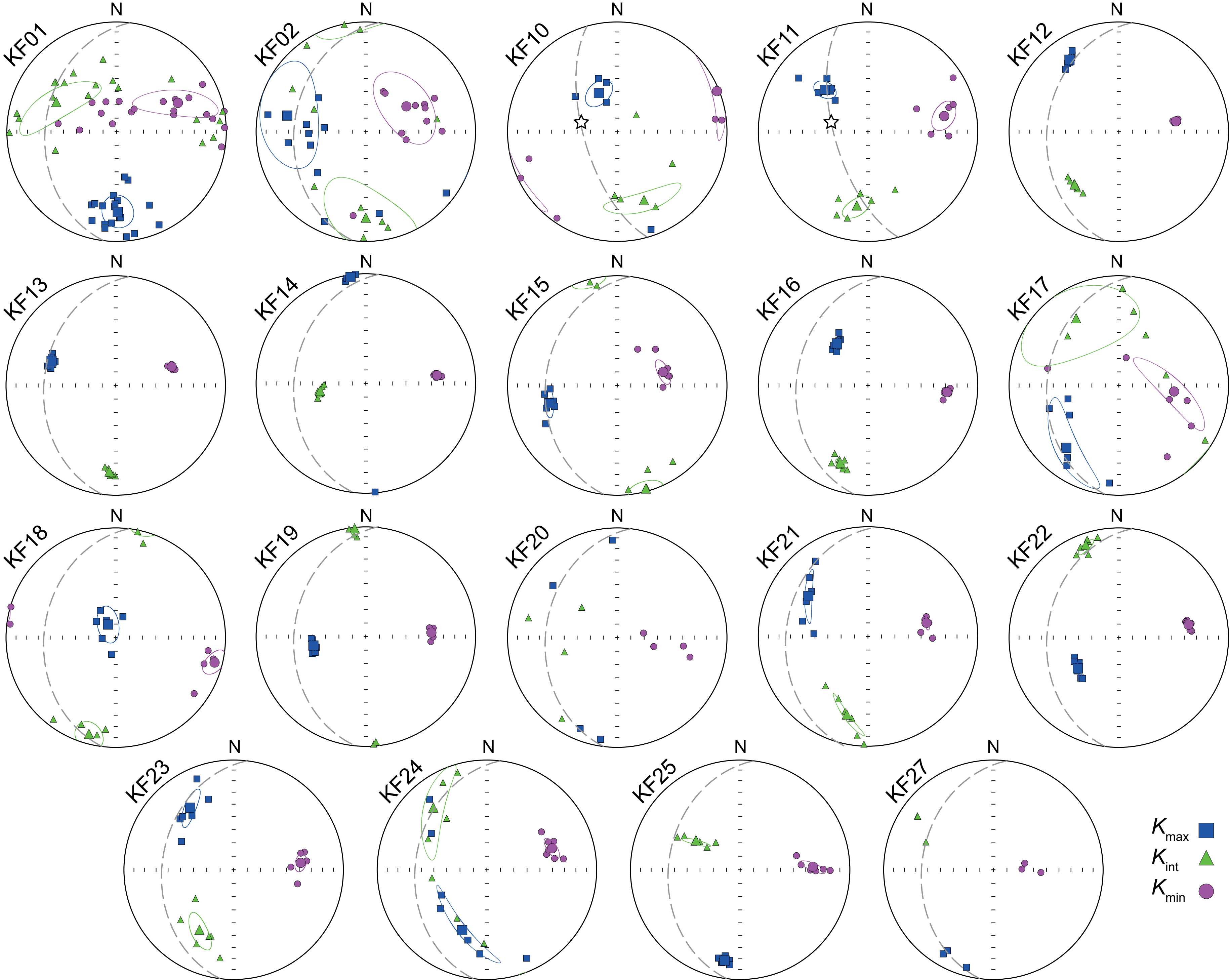

N
KF01
KF02
KF10
KF11
KF12
KF13
KF14
KF15
KF16
KF17
KF18
KF19
KF20
KF21
KF22
KF23
KF24
KF25
KF27
K_{max}
K_{int}
K_{min}

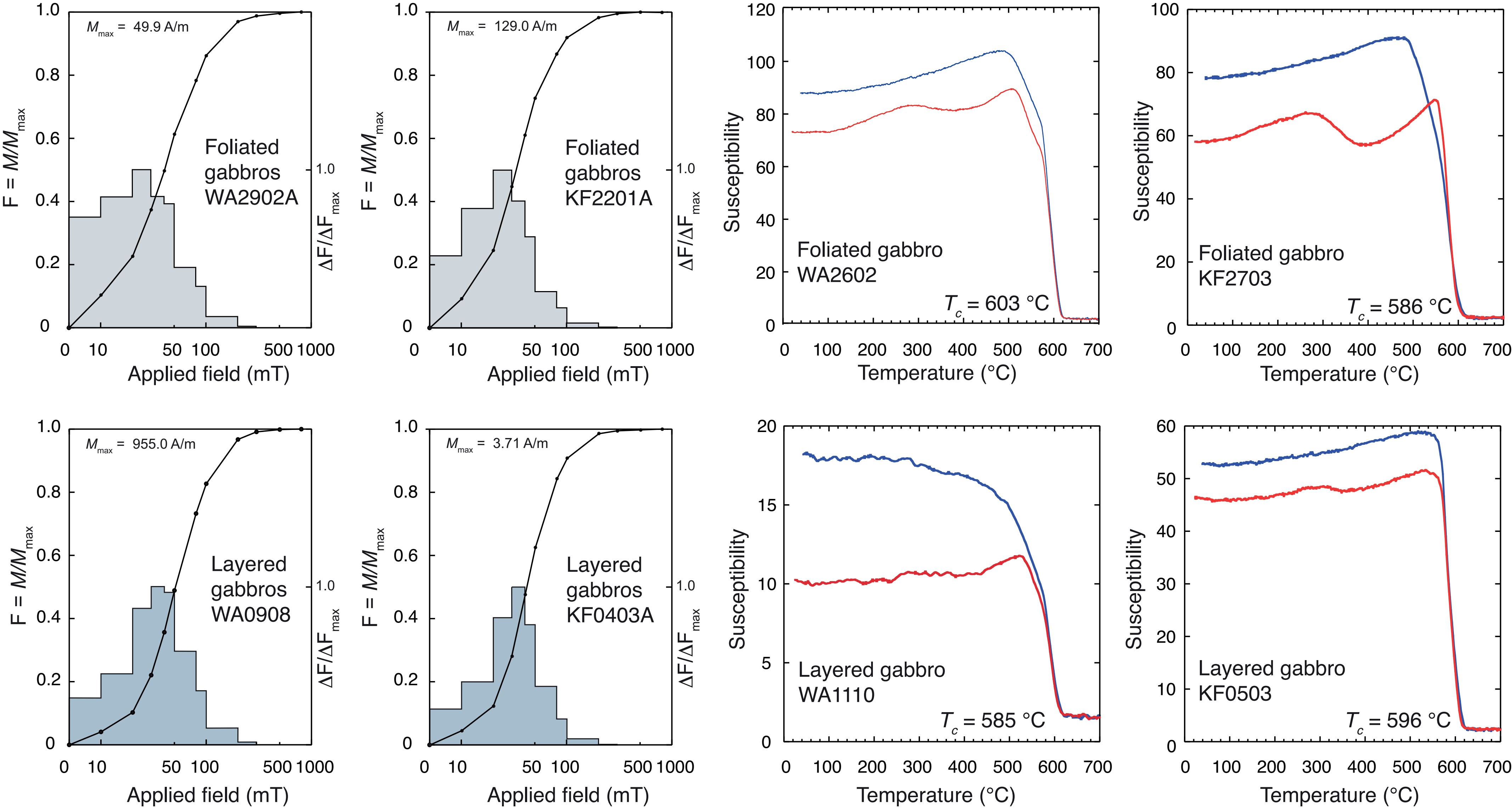

M_{max} = 49.9 A/m
Foliated gabbros WA2902A
M_{max} = 129.0 A/m
Foliated gabbros KF2201A
Foliated gabbro WA2602
T_c = 603 °C
Foliated gabbro KF2703
T_c = 586 °C
M_{max} = 955.0 A/m
Layered gabbros WA0908
M_{max} = 3.71 A/m
Layered gabbros KF0403A
Layered gabbro WA1110
T_c = 585 °C
Layered gabbro KF0503
T_c = 596 °C
F = M/M_{max}
$\Delta F/\Delta F_{max}$
Applied field (mT)
Susceptibility
Temperature (°C)

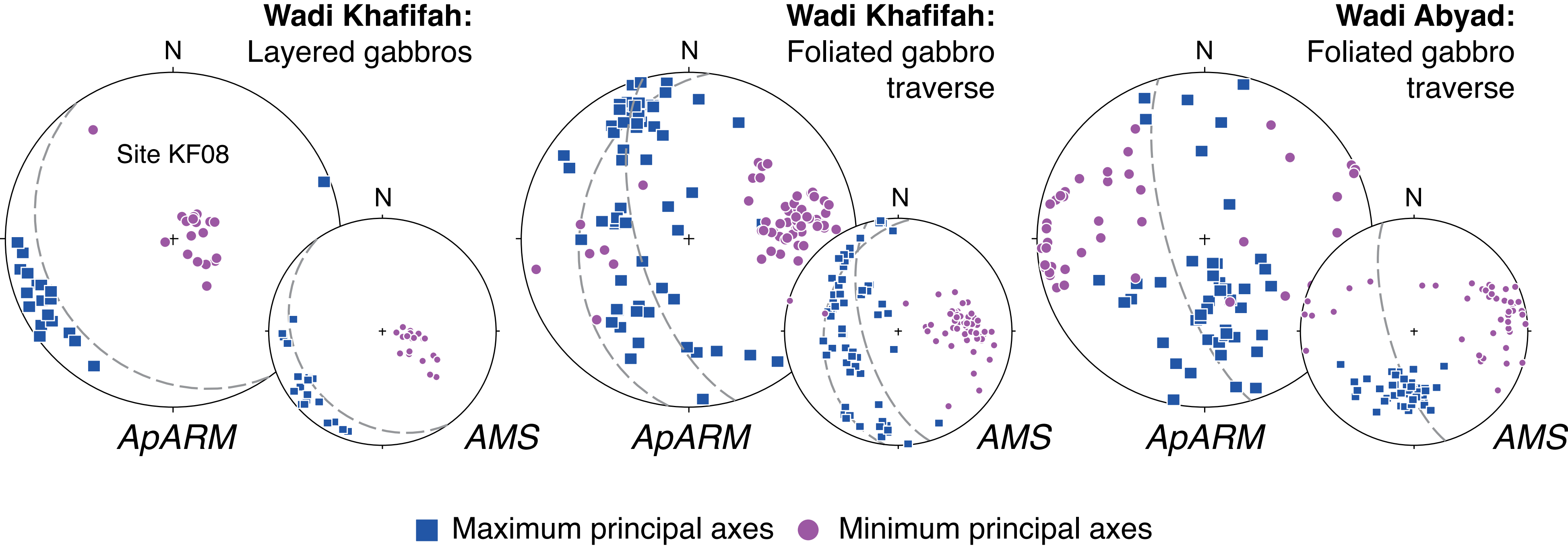
Wadi Khafifah:
Layered gabbros
N
Site KF08
ApARM
N
AMS
Wadi Khafifah:
Foliated gabbro
traverse
N
ApARM
N
AMS
Wadi Abyad:
Foliated gabbro
traverse
N
ApARM
N
AMS
Maximum principal axes
Minimum principal axes